Eur. Phys. J. B **57**, 109–113 (2007)
DOI: 10.1140/epjb/e2007-00161-0

THE EUROPEAN PHYSICAL JOURNAL B

Kauffman networks with threshold functions

F. Greil[a] and B. Drossel

Institut für Festkörperphysik, Technische Universität Darmstadt, Hochschulstraße 6, 64289 Darmstadt, Germany

Received 24 February 2007 / Received in final form 24 April 2007
Published online 1st June 2007 –

Abstract. We investigate Threshold Random Boolean Networks with $K = 2$ inputs per node, which are equivalent to Kauffman networks, with only part of the canalyzing functions as update functions. According to the simplest consideration these networks should be critical but it turns out that they show a rich variety of behaviors, including periodic and chaotic oscillations. The analytical results are supported by computer simulations.

PACS. 89.75.Hc Networks and genealogical trees – 05.70.Fh Phase transitions: general studies – 05.65.+b Self-organized systems

1 Introduction

Random Boolean networks (RBN) were introduced by Stuart Kauffman in 1969 [1,2] to model the dynamics of genetic and metabolic networks [3], but they are also used in a social and economic context [4,5], and for neural networks. Although Boolean models represent a strong simplification of the far more complex reality, there exist several examples where the modelling of a genetic network by Boolean variables captures correctly the essential dynamics of the system [6–8]. For this reason, the study of RBNs remains an important step on the way towards understanding real networks.

In a RBN, the nodes have only two possible states, "on" and "off". Each node is assigned at random a set of nodes from which it receives its inputs, and an updating rule. All nodes are updated in parallel. Kauffman classified the dynamics of RBNs according to whether it is *chaotic* or *frozen* or *critical* (as described in the review [9]).

1. In a frozen network, all nodes apart from a small number (that remains finite in the limit of infinite system size) assume a constant value after a transient time. If two identical systems are started in a different initial state, the states of all nodes apart from a finite number become identical after the transient time. If in the stationary state the value of one node is changed, this perturbation propagates during one time step on average to less than one other node.
2. In a chaotic network, attractors of the dynamics are long, and a nonvanishing proportion of all nodes keep changing their state even after long times. If two identical systems are started in a different initial state, the states of a nonvanishing proportion of all nodes remain different even after long times. If in the stationary state the value of one node is changed, this perturbation propagates during one time step on average to more than one other node.
3. Critical networks are at the boundary between these two types of behavior, with a perturbation of one node propagating on average to one other node. Therefore the difference between two almost identical initial states increases like a power law in time. The number of nodes that are not frozen on all attractors increases in a critical network as a power law $\sim N^{2/3}$ of the system size N, as was found numerically in [10] and analytically in [11,12].

This simple classification was made for networks in which all possible Boolean functions occur. The mean-field calculation that is usually performed for deciding to which class a network belongs, is based on the assumption that the proportion of nodes in the "on" (or "off") state becomes a constant for long times.

However, this need not be the case. In fact, for some types of Boolean networks the proportion of nodes in the "on" state has been shown to display more complicated temporal behaviour. When a parameter is varied, period-doubling cascades and chaos are found in networks where all nodes with the same number of inputs are assigned the same Boolean function [13–15].

In this paper, we want to build a bridge between RBNs with constant proportions of "on" nodes, and between Boolean networks with only one type of functions and more complicated dynamics of the proportion of "on" nodes. We study a rather simple class of RBNs and investigate in more detail its dynamical behaviour. In our networks, there occur different Boolean functions, the weights of which can be varied by tuning a parameter. We do not only study the time evolution of the number of "on" nodes,

[a] e-mail: florian.greil@physik.tu-darmstadt.de

but also the attractors of the networks. We find a frozen and a chaotic phase (according to Kauffman's classification), and a regime with an oscillation of period 2 in the number of "on" nodes. Interestingly, within this regime, there is an additional phase transition from a phase with attractors of period 2 to a phase with very long attractors. Our results indicate that the dynamics of RBNs are in general much richer than what has been reported so far.

1.1 The model

We model a random Boolean network as a directed graph with randomly chosen links between N binary nodes, each of which has K inputs. We denote the state of a node with $\sigma_i = \pm 1$ (we call $+1$ "on" and -1 "off"). Each node i is assigned at random an update function f_i. In this paper, we focus on the case $K = 2$ and on threshold functions

$$f_i = \text{sign}\left(h + \sum_j \sigma_j c_{ij}\right) \equiv \text{sign}\,(s_i) \qquad (1)$$

where the sum is taken over the two input nodes for node i. The value $c_{ij} = -1$ stands for *inhibitory* connections and $c_{ij} = 1$ for *excitatory* connections. (This version of RBN was used for instance in [16] with a threshold value $h = 0$.) A connection is excitatory with probability p_+ and inhibitory with probability $1 - p_+$. We set the value of the threshold to $h = 0$. Since each of the two input connections can be excitatory or inhibitory, the model has 4 different update functions, which are listed in Table 1 together with their weights.

In agreement with other authors, we define $\text{sign}(0) = 1$. Threshold functions are used not only in the context of neural networks, but also in models for markets [17] and for genetic networks [7,16,18]. The functions listed in Table 1 represent four of the 12 canalizing update functions of Kauffman networks. Canalyzing functions are those non-frozen functions where at least one value of a given input can fix the output of a node, irrespective of the value of the second input. All nodes are updated in parallel according to the rule

$$\sigma_i(t+1) = f_i(\{\sigma_j(t)\}) \equiv f_i(\sigma_{i_1}(t), \sigma_{i_2}(t)). \qquad (2)$$

Node i depends on the nodes j, namely on node i_1 and i_2. The functions used in this paper are a subset of those classified as *biological meaningful* by Raeymakers [19].

The configuration of the system $\boldsymbol{\sigma} \equiv \{\sigma_1, \ldots, \sigma_N\}$ performs a trajectory in configuration space. As the state space is finite and the dynamics is discrete, some states will occur again. If a *cycle* in state space has a set of transient states leading to it, it is called an *attractor*.

2 Classification of the dynamics according to Kauffman

We will now apply the classification rule of Kauffman to our threshold networks. Then we will show that this classification breaks down for a certain range of values of the parameter p_+, and we will study in the next section in more detail this parameter range, were global oscillations occur.

Table 1. The four possible update functions for the model used in this paper. The input configuration is given in the first column, with $\uparrow$ denoting $\sigma_i = 1$ and $\downarrow$ denoting $\sigma_i = -1$. The top row gives the name of the function according to the Kauffman model, the last row gives the probability for each function.

Input	f_7	f_{11}	f_{13}	f_{14}
$(\downarrow,\downarrow)$	$\uparrow$	$\uparrow$	$\uparrow$	$\downarrow$
$(\downarrow,\uparrow)$	$\uparrow$	$\uparrow$	$\downarrow$	$\uparrow$
$(\uparrow,\downarrow)$	$\uparrow$	$\downarrow$	$\uparrow$	$\uparrow$
$(\uparrow,\uparrow)$	$\downarrow$	$\uparrow$	$\uparrow$	$\uparrow$
probability	$(1-p_+)^2$	$p_+(1-p_+)$	$p_+(1-p_+)$	p_+^2

Let us first apply the criticality condition in its simplest version: for all four update functions, the probability that the output changes if one input spin is flipped, is 1/2. Since each node is on average the input to two other nodes, a perturbation at one node propagates on average to one other node, and we should expect the model to be critical. This is in agreement with the finding that $K = 2$-RBNs that contain only canalyzing update functions (but all of them with the same probability) are critical [20]. However, this simple argument is based on the assumption that all four possible input configurations occur equally often, which may be true at the beginning of a simulation run, but may be wrong already after one timestep. For this reason, Moreira and Amaral [21] argued that the calculation should be performed such that the input configurations are weighted with their frequencies in the stationary state. This type of calculation is explained in great detail in [22]. A similar type of calculation was applied already earlier to a lattice model, where the approximation is not exact [23].

2.1 Perturbation propagation method

Let us therefore next apply the rule given by Moreira and Amaral and let us determine for what values of p_+ it predicts that the model is frozen, critical, or chaotic.

We denote with b_t the proportion of nodes in state $\sigma_i = +1$ at time t. In the thermodynamic limit, it changes deterministically according to

$$b_{t+1} = 1 - \left[b_t^2\,(1-p_+)^2 + (1-b_t)^2\,p_+^2 + 2b_t\,(1-b_t)\,p_+\,(1-p_+)\right]. \qquad (3)$$

The expression in the square brackets is the probability that an input combination leads to $s_i = -2$, which yields an output -1. In the stationary state, we have $b_{t+1} = b_t = b$ with

$$b(p_+) = \frac{4p_+^2 - 2p_+ - 1 \pm \sqrt{5 - 12p_+ + 8p_+^2}}{2(1-2p_+)^2}. \qquad (4)$$

The sign in the numerator has to be chosen such that $b \in [0,1]$, therefore only the positive branch remains, see Figure 1. For $p_+ = 1/2$, the denominator vanishes, and the stationary solution of equation (3) is $b = 3/4$. For $p_+ = 1$, we have $b = 0$ and $b = 1$, with the first solution being obviously unstable as it is destroyed by one node in the state $\sigma_i = +1$. The second solution is a stable fixed point of the dynamics. For $p_+ = 0$, we have $b = (-1+\sqrt{5})/2$.

The mean number of nodes to which a perturbation at one node propagates is in the stationary state given by $2\pi_1$, with π_1 being the probability that a node changes its state when one input is flipped. We obtain it by adding together the probabilities for those input configurations which allow a transition between an output $+1$ and -1 and vice versa. This is true for half of the input configurations leading to $s_i = 0$ (the first 4 terms in the following equation) and for all input configurations for which $s_i = -2$ (the last 4 terms):

$$\begin{aligned}\pi_1 = &(1-p_+)(1-b)(1-p_+)b + p_+bp_+(1-b)\\ &+p_+b(1-p_+)b + (1-p_+)(1-b)p_+(1-b)\\ &+(1-p_+)b(1-p_+)b + p_+b(1-p_+)(1-b)\\ &+(1-p_+)(1-b)p_+b + p_+(1-b)p_+(1-b)\\ \Rightarrow \pi_1 = &\, b + p_+ - 2bp_+. \end{aligned} \tag{5}$$

For $p_+ = 1/2$, we obtain $\pi_1 = 1/2$, for $p_+ = 1$, we obtain $\pi_1 = 0$. For $p_+ = 0$, we obtain $\pi_1 = b \simeq 0.618$. We therefore conclude that the model is in the frozen phase for $p_+ > 1/2$, that it is critical for $p_+ = 1/2$, and chaotic for $p_+ < 1/2$.

2.2 Stationarity method

The same result is obtained by calculating the stationary value of the Hamming distance between two identical network realizations. The (normalized) Hamming distance between two configurations $\boldsymbol{\sigma}, \tilde{\boldsymbol{\sigma}}$ is the fraction of nodes that have different values in the two configurations: $D = (4N)^{-1}\sum_{i=1}^{N}(\sigma_i - \tilde{\sigma}_i)^2$. If we denote with π_2 the probability that a node changes its state when both inputs are flipped, the time evolution of D is given by

$$D_{t+1} = 2D_t(1-D_t)\pi_1 + D_t^2\pi_2. \tag{6}$$

The first term is the probability that exactly one input changes, times the probability that the output flips. The second term is the probability that both inputs change, times the probability that the output flips.

The value of π_2 in the stationary state is obtained by summing all 8 combinations leading to $s_i \in \{\pm 2\}$. It can be written as

$$\pi_2 = 1 - 2b(1-2p_+)^2 + 2b^2(1-2p_+)^2 - 2p_+ + 2p_+^2 \tag{7}$$

and is $1/2$ for $p_+ = 1/2$ and 1 for $p_+ = 1$. If D_t is very small, we have

$$D_{t+1} \simeq 2D_t\pi_1, \tag{8}$$

which allows for the growth of a small perturbation if $2\pi_1 > 1$ or $p_+ < 1/2$, in agreement with our result above.

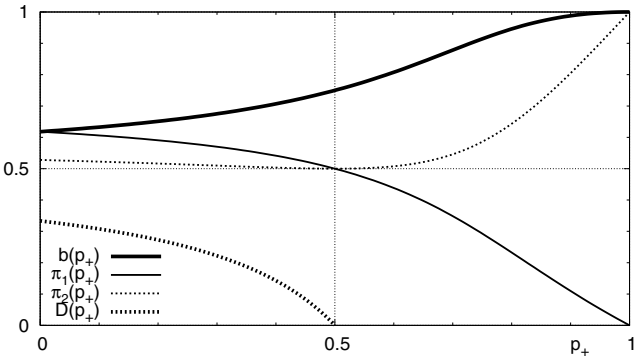

Fig. 1. The functions $b(p_+), \pi_1(p_+), \pi_2(p_+)$ and the stationary value $D(p_+)$ vs. p_+.

The transition from a stationary value $D = 0$ to a stationary value $D > 0$ occurs at the same point.

Figure 2 shows D_t for different values of p_+ and for given initial conditions. One can see that D_t approaches 0 for large times if $p_+ > 0.5$. Furthermore, one can see that D_t oscillates with period 2 for the smaller values of p_+. This oscillation is an indication that the dynamics in the "chaotic" phase has some structure, which shall be investigated in the following.

3 The nonfrozen regime

Let us have a closer look at the phase that was classified above as chaotic based on the evaluation of π_1 at the fixed point value of b. In fact, the dynamics is not chaotic at all for sufficiently small p_+. The reason is that our calculations were based on the assumption that b becomes stationary for large times. In order to see that this need not be the case, let us first look at the situation where $p_+ = 0$: We then have $b_{t+1} = 1 - b_t^2$. This is a one-dimensional map shown in Figure 3.

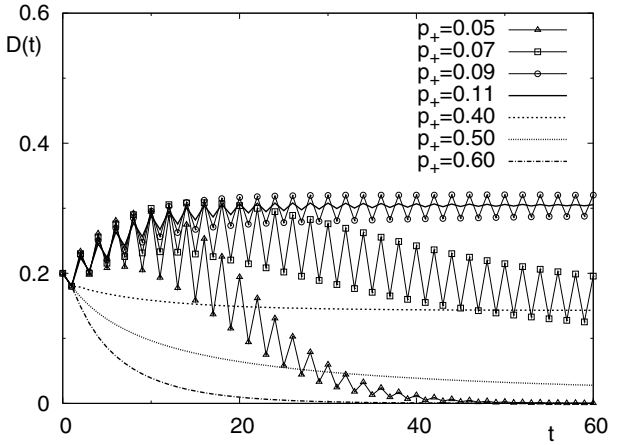

Fig. 2. The time evolution of the Hamming distance D for different values of p_+ when b is not stationary. The curves are calculated according to equations (3, 6) starting from $D_0 = 0.2$ and $b_0 = 0.5$.

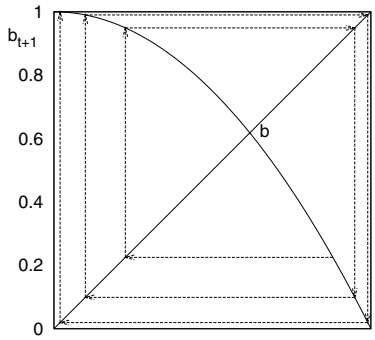

Fig. 3. The map b_t vs. $b_{t+1} = 1 - b_t^2$ for $p_+ = 0$. The fixed point b is unstable as depicted by a sample trajectory.

The fixed point is unstable, just as is found in specific RBN models where all nodes are assigned the same function [13]. Instead of having a stationary point with a constant proportion of nodes in the two states, the system oscillates between a configuration where all nodes are switched on and a state where all nodes are switched off. This is not chaotic dynamics at all, but very stable dynamics. In order to determine the range of p_+values, for which the fixed point value of b is unstable, we performed a linear stability analysis. The ansatz $b_{t+1}(b+\delta b_t) = b+\delta b_{t+1}$ leads in linear order in δb and for $p_+ < 1/2$ to

$$\begin{aligned}\delta b_{t+1} &= -2\left(b_t\left(1-2p_+\right)^2 + \left(1-2p_+\right)p_+\right)\delta b_t \\ &= \left(1-\sqrt{5-12p_+ + 8p_+^2}\right)\delta b_t =: M\cdot\delta b_t. \end{aligned} \quad (9)$$

In the last step we used equation (4). The fixed point is stable if the real part of M is smaller than 1, which is the case if

$$p_+ > (3-\sqrt{7})/4 \equiv p_{cb} \approx 0.0886. \quad (10)$$

Only above this value does the system have a stationary state with constant proportions of nodes being "on" and "off".

3.1 Oscillations with period 2

We finally investigate in more detail the region $p_+ < p_{cb}$, where the proportion of "on" and "off" nodes oscillates with period 2. For $p_+ = 0$, every node oscillates with period 2, and we have a global attractor of period 2. This need not necessarily be the case if b oscillates with period 2. The attractor could be much larger, while the proportion of off and on nodes oscillates still with period two. In order to determine for which parameters an attractor with period 2 is stable, we performed again a linear stability analysis, but now for two time steps together. We assume that the system is on an attractor of length 2. Let there be every even time step a proportion x of "on"-nodes and every odd step a proportion y.

We flip one node and evaluate how the Hamming distance grows in comparison to the undisturbed system after two time steps. The condition that a perturbation of one node propagates on average to one other node after two time steps is equivalent to

$$\pi_1(x)\cdot\pi_1(y) = \frac{1}{4}. \quad (11)$$

Combining equation (11) with the time evolution of x and y as given by equation (3), we obtain three equations

$$\begin{aligned} y &= 1-[x^2(1-p_+)^2 + (1-x)^2p_+^2 + 2x(1-x)p_+(1-p_+)] \\ x &= 1-[y^2(1-p_+)^2 + (1-y)^2p_+^2 + 2y(1-y)p_+(1-p_+)] \\ \frac{1}{4} &= (x+p_+-2xp_+)(y+p_+-2yp_+). \end{aligned}$$

This system can be solved numerically, and we obtain a critical value $p_{cn} = 0.0657$. For p_+ below this value a perturbation at one node will die out and all nodes will again oscillate with period 2. Above this value, attractors must be longer than 2.

3.2 Numerical test

We checked these analytical predictions by performing computer simulations. In order to identify the transition at p_{cn}, we measured the median attractor length. As shown in Figure 4, we find with increasing network size an increasingly sharp transition. Below the transition at p_{cn}, the proportion of attractors of length 2 converges to some nonzero value with increasing system size, indicating that cycles of length 2 are stable. Above the transition, the median attractor length increases more and more rapidly with increasing system size, indicating a diverging median. Another finding is that attractors become again shorter as the critical point $p_+ = 1/2$ is approached.

The transition at p_{cb} is a transition from oscillating to stationary behavior of b_t, which we have obtained in the analytical calculation at the beginning of this chapter. In order to see this transition also in our computer simulation, we evaluated the frequency of phase jumps in b_t on the attractors. An oscillation with period 2 was identified by observing that the value of b_t alternated between being larger and smaller than its mean value $\langle b\rangle$. Deviations from this regular oscillation are "phase jumps", where b_t is two times in a row above or below the mean value. A finite proportion of phase jumps means that the regular oscillation with period 2 ceases to exist and that the point p_{cb} has been reached. The result is shown in the lower part of Figure 4. With increasing system size, there is an increasingly sharp transition at p_{cb} between zero phase jumps and a finite proportion of phase jumps. In order to verify that b becomes stationary above the transition, we also evaluated its standard deviation Δb. We find that Δb decreases with increasing system size above p_{cb} while it increases below the transition. For instance, for networks with only 100 nodes we obtained $\Delta b < 0.1$ for $p_+ > 0.15$. This finding agrees with our analytical result that b is constant in time above p_{cb}.

4 Conclusion

To conclude, we have shown that the simplest Threshold Random Boolean Network shows three different types

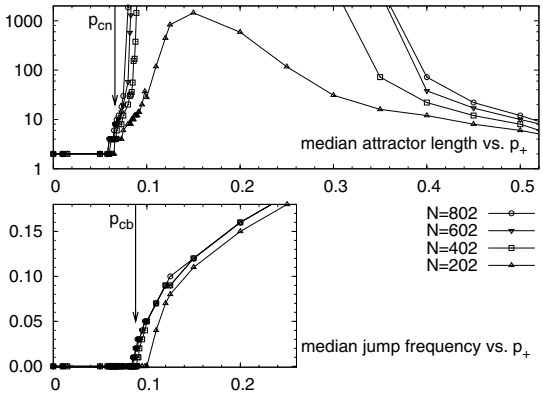

Fig. 4. Numerical verification for the transition p_{cn} and p_{cb}, both marked by vertical arrows. The upper panel shows the median attractor length, the lower panel the median frequency of phase jumps on each attractor candidate in dependence of p_+. Each data point corresponds to 5000 sample networks of size N with fixed p_+ and two initial conditions per realization. Sampling the entire state space is impossible already for networks much smaller than the N considered here. This means that attractors are weighted with the size of their basin of attraction. The time evolution is limited to 5000 computational steps for both the transient and the attractor length, in order to keep the overall simulation time within reasonable limits. This makes it impossible to calculate mean attractor lengths, therefore the median was evaluated.

of phase transitions and not just the generally expected transition between a frozen and a chaotic phase. For parameter values $p_+ < p_{cn}$, all nodes oscillate stably with period two. For $p_{cn} < p_+ < p_{cb}$, the fraction of on-nodes oscillate with period two, but attractors are longer. For $p_{cb} < p_+ < 1/2$, the dynamical behavior is chaotic in the sense defined by Kauffman. For $p_+ > 1/2$, the network is in the frozen phase.

We summarize the different types of dynamical behavior in the following diagram, Figure 5.

nonfrozen			frozen
b has period 2		b is constant in time	
all nodes have period 2	nodes oscillate differently or not at all		

p_+ p_{cn} p_{cb} 0.5

Fig. 5. Overview of the dynamic behavior of the model with $K = 2$ in dependence of the parameter p_+.

The lesson to be learned from this study is that the dynamical behavior of RBNs can be much richer than expected from simple considerations. Some RBNs may show global oscillations with higher periods or period doubling cascades in the temporal behavior of b_t, as was found in special networks where all nodes with the same number of inputs are assigned the same function. Even more interestingly, within a regime with a fixed oscillation period of the number of "on" nodes, further phase transitions can be hidden, as we have seen in this paper.

Real genetic networks might therefore also have a richer dynamical behaviour than the dynamical classes identified by Kauffman. If the simple classification into "frozen", "critical" and "chaotic" networks fails already in the random threshold model presented in this paper, it will be even less suitable for real genetic networks, which have attractors with very specific properties related to the function of the network. Also a characterization by the temporal behaviour of the proportion of "on" nodes will not be sufficient. A more sophisticated way of describing and classifying the dynamical behavior of Boolean networks is therefore required.

This work was supported by the Deutsche Forschungsgemeinschaft (DFG) under Contract No. Dr200/4-1.

References

1. S.A. Kauffman, J. Theo. Bio. **22**, 437 (1969)
2. S. Kauffman, Nature **224**, 177 (1969)
3. S. Kauffman, C. Peterson, B. Samuelsson, C. Troein, Proc. Nat. Acad. Sci. **100**, 14796 (2003), e-print arXiv:q-bio.MN/0412005
4. J.M. Alexander, in *Philosophy of Science Assoc. 18th Biennial Mtg.* December 10th, 2002
5. M. Paczuski, K.E. Bassler, A. Corral, Phys. Rev. Lett. **84**, 3185 (2000), e-print arXiv:cond-mat/9905082
6. S. Bornholdt, Science **310**, 449 (2005)
7. F. Li, T. Long, Y. Lu, Q. Ouyang, C. Tang, Proc. Nat. Acad. Sci. **101**, 4781 (2004), e-print arXiv:q-bio.MN/0310010
8. R. Albert, H.G. Othmer, J. Theo. Biol. **223**, 1 (2003), e-print arXiv:q-bio.MN/0311019
9. M. Aldana-Gonzalez, S. Coppersmith, L.P. Kadanoff, *Perspectives and Problems in Nonlinear Science* (2003), pp. 23–89, e-print arXiv:nlin.AO/0204062
10. J.E.S. Socolar, S.A. Kauffman, Phys. Rev. Lett. **90**, 068702 (2003), e-print arXiv:cond-mat/0212306
11. B. Samuelsson, C. Troein, Phys. Rev. Lett. **90**, 098701 (2003), e-print arXiv:cond-mat/0211020
12. V. Kaufman, T. Mihaljev, B. Drossel, Phys. Rev. E **72**, 046124 (2005), e-print arXiv:cond-mat/0506807
13. M. Andrecut, M.K. Ali, Int. J. Mod. Phys. B **15**, 17 (2001)
14. M.T. Matache, J. Heidel, Phys. Rev. E **69**, 056214 (2004)
15. M. Andrecut, J. Stat. Mech. **2**, P02003 (2005)
16. T. Rohlf, S. Bornholdt, Physica A **310**, 245 (2002), e-print arXiv:cond-mat/0201079
17. D. Stauffer, G. Weisbuch, Int. J. Mod. Phys. B **17**, 5495 (2003)
18. S. Bornholdt, K. Sneppen, Proc. R. Soc. London B **267**, 2281 (2000), e-print arXiv:cond-mat/0003333
19. L. Raeymaekers, J. Theo. Bio. **218**, 331 (2002)
20. U. Paul, V. Kaufman, B. Drossel, Phys. Rev. E **73**, 026118 (2006), e-print arXiv:cond-mat/0511049
21. A.A. Moreira, L.A.N. Amaral, Phys. Rev. Lett. **94**, 218702 (2005), e-print arXiv:cond-mat/0504722
22. J. Kesseli, P. Rämö, O. Yli-Harja, Phys. Rev. E 046104 (2006)
23. W.K. Wootters, C.G. Langton, Physica D **95**, 95 (1990)